

Review

Recent Application of Metal-Organic Frameworks in an Electrochemical Immunosensor

Chenyu Dai^{1,†}, Yuefeng Zhao^{1,†}, Peiwu Chen¹, Jinyao Liu¹, Caihong Wang¹, Lan Jiang¹, Ying Huang¹, Meina Feng¹, Ruizhuo Ouyang^{1,*}, Yuqiang Miao¹, Shuang Zhou^{2,*}

¹ Institute of Bismuth and Rhenium Science, School of Materials and Chemistry, University of Shanghai for Science and Technology, Shanghai, 200093, China

² Cancer Institute, Tongji University School of Medicine, Shanghai, 200092, China

*E-mail: ouyangrz@usst.edu.cn

[†]Contributed equally to this study as co-first authors.

Received: 11 February 2022 / Accepted: 11 March 2022 / Published: 5 April 2022

An electrochemical immunosensor combines electrochemical technology with an immune response to disease biomarkers with characteristics of high sensitivity, simple instrumentation, and flexible methods. Metal-organic frameworks (MOFs) belong to a class of porous materials with a periodic crystalline network structure. Generally, the metal ions in MOFs are electrochemically active. MOFs have well-ordered pores and a large specific surface area, which makes it easy to immobilize antibodies, promoting the application of MOFs in electrochemical immunosensors whose selectivity toward targeted proteins and bacteria can be greatly improved through introducing antigens or antibodies inside MOFs. MOFs have been regarded as promising carriers to effectively increase antibody loading; they sometimes showed favorable enzyme-like catalytic activity as well. In this review, we first introduced the response forms of electrochemical immunosensors, followed by the discussion of the application of MOFs in electrochemical immunosensors in the last 5 years based on the six electrochemical detection methods. Some important prospects and further challenges in this area were briefly discussed in the end.

Keywords: Biomarkers; detection; electrochemical immunosensors; Metal organic Frameworks MOFs

1. INTRODUCTION

The incidence of cancer, which is known as one of the three major health killers threatening humanity in the 21st century, has increased in recent years.[1] In fact, any changes in normal cells can be marked by abnormal expression of certain biomolecules due to their interrelated functions. The significant abnormalities within these biomolecules can enable the diagnosis of diseases at a very early stage. [2] thus greatly promoting the application of biosensors in medicine. Besides, biosensors can also be used for food composition analysis, pesticide residue analysis, and water environment detection.

According to the International Union of Pure and Applied Chemistry, a biosensor is defined as a device using specific biochemical reactions mediated by isolated enzymes, immunosystems, tissues, organelles, or whole cells for the detection of chemical compounds usually by electrochemical, optical or thermal signals.[3] Biosensors can be used to detect enzymes,[4] antibodies,[5], peptides,[6] aptamers,[7] and DNA[8] according to biological receptors, as shown in Figure 1. Antibodies are immunoglobulins produced by the human body due to the stimulation of the antigens; they can specifically bind to the antigens. The most common principle of immunosensors is antigen–antibody interactions,[9] as the binding of antigen and antibody has high specificity, reduced nonspecific interference, high sensitivity, high specificity, and high stability.[10-11] The types of immunosensors include electrochemical,[12] optical,[13] surface plasmon resonance [14]. The reason why an electrochemical immunosensor stands out among them is that the electrochemical detection equipment is simple, portable, and fast, and can easily realize the trace detection of actual samples.[15]

In recent years, metal-organic framework (MOF) materials are new, highly porous crystal materials, which are self-assembled via coordination bonds through inorganic metal nodes and organic ligands.[16-17] Compared with conventional ceramic porous materials,[18] plastic porous materials,[19] and carbon materials,[20] MOF materials have unique advantages and are promising in the field of sensors. MOFs have dramatically attracted the increasing attention of scientists and engineers due to their highly ordered material structure and pore properties and the simple preparation method. The highly ordered pore size and the large specific surface area of MOFs are suitable for anchoring enzymes, antibodies, and other biomolecules by van der Waals force, π - π interaction, hydrogen bonding, and hydrophobic or electrostatic interaction. According to the different organic ligands, amino and carboxyl functional groups can be modified outside MOFs to make MOFs an ideal immobilization matrix for immobilizing biomolecules through covalent bonding.[21-22] Because of these advantages, the design of highly stable and specific immunosensors based on MOFs has become a hot topic in recent years.

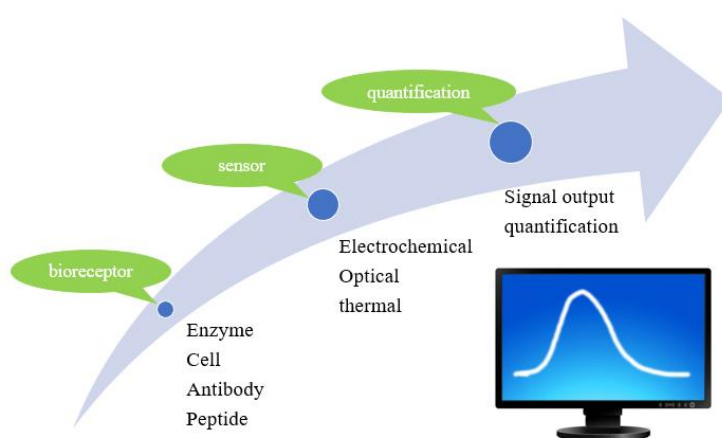


Figure 1. Signal response principle of biosensors.

In this review, we summarized different kinds of MOF-based electrochemical immunosensors. First, we introduced the basic response forms of electrochemical immunosensors: competitive,

sandwich, and direct, followed by six electrochemical detection methods of electrochemiluminescence (ECL), differential pulse voltammetry (DPV), square wave voltammetry (SWV), electrochemical impedance spectroscopy (EIS), amperometry, and conductimetry in MOF-based electrochemical immunosensors. Based on the aforementioned information, the development prospects and challenges of MOFs in the field of electrochemical immunosensors were outlined.

2. ELECTROCHEMICAL IMMUNOSENSORS

Electrochemical immunosensors are usually divided into two types: label and label-free. The former includes competitive and sandwich methods. The competitive type is used to detect small-molecule antigens that cannot bind to two antibodies at the same time. This includes direct and indirect forms. The direct competition method fixes the antibody on the surface of electrode, and the labeled antigen competes with the free antigen. Labeled antibodies compete with free antibodies. Usually, the second method is chosen to avoid the problems associated with antibody fixation (correct antibody orientation and loss of affinity). The sandwich-type is used to detect a large-molecule antigen or antibody. After the antigen is bound to the antibody immobilized on the electrode surface, a labeled antibody directed to a second binding site of the antigen is added. The labeled antigen/antibody is captured by the detection target, and the redox current change of the label can be detected. Hence, this method is more sensitive than the unlabeled method. MOF materials are mainly used as labeled carriers of enzymes or quantum dots in labeled electrochemical immunosensors; they play an enzyme-like catalytic role and serve as immobilized antibodies.

Label-free immunosensors perform quantitative analysis directly by immobilizing antibodies on electrodes and based on the current, resistance, and potential changes caused by antibody–antigen-specific reactions. The high specific surface area and electrical activity of some MOF materials can immobilize sufficient antibodies and amplify the electrochemical response signal of the immune interaction.

Regardless of whether they are marked or unmarked, their basic principles are similar: capture analysis (usually antigen), blocking unreacted surfaces, and identification analysis.[23]

2.1 Detection of electrochemiluminescence (ECL)

ECL is the chemical reaction of a specific substance caused by an electrochemical reaction on the electrode surface; the biomarker is quantitatively analyzed by the luminous intensity of the substance. Most ECL immunosensors use signal-quenched mode, also known as "signal-off" for better sensitivity and lower limit of detections (LODs). The premise of obtaining high sensitivity is that the stable and strong initial ECL signal, and an effective signal amplification strategy is paramount.[24]

The conventional ECL luminophores, such as Tris(2,2'-bipyridyl) ruthenium(II) ($\text{Ru}(\text{Bpy})_3^{2+}$) and its derivatives, have the advantages of electroluminescence efficiency and good biocompatibility. However, $\text{Ru}(\text{Bpy})_3^{2+}$ is water soluble and cannot be used alone. To avoid the partial quenching of $\text{Ru}(\text{Bpy})_3^{2+}$ in an aqueous solution, nanocarriers can be constructed to encapsulate $\text{Ru}(\text{Bpy})_3^{2+}$ by

electrostatic incorporation.[25] Dong designed an ECL immunosensor for detecting diethylstilbestrol (DES) based on the competitive method. The increase of DES concentration in the human body can cause potential deformities and cancer risk.[26] Taking advantage of the huge equivalent internal surface area of MOFs, Ru(Bpy)₃²⁺ was encapsulated in MOFs UiO-67, forming UiO-67-Ru(Bpy)₃²⁺ used as a marker and labeled on the bovine serum albumin–DES (BSA-DES), which competed with DES for estimating the DES content. During the detection of DES, the binding of labeled BSA-DES to antibodies and the ECL signal gradually decreased, thereby achieving the purpose of determining DES content. A wide linear range was received with this immunosensor from 0.01 pg/mL to 50 ng/mL with a LOD as low as 3.27 fg/mL at a signal-to-noise ratio of 3 (S/N = 3). The interference of aflatoxin B1, prostate-specific antigen, human serum albumin, and alpha-fetoprotein had little effect on the detection of DES (Fig. 2).[27]

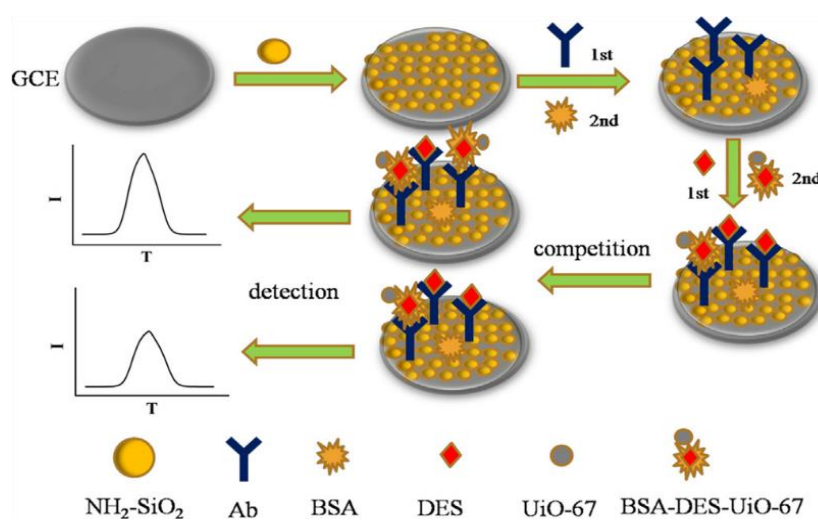


Figure 2. Schematic diagram for the electrochromescence immunosensor fabrication.[27] Copyright 2018 Elsevier.

The high dose of deoxynivalenol (DON), as a member of the mycotoxin family, causes diarrhea and vomiting in animals.[28] Zheng used MOF MIL-125(Ti) to immobilize enough Ru(Bpy)₃²⁺ and mercapto-beta-cyclodextrin (β -CD). Fluoro-coumarin silicon (IV) phthalocyanine (F-couSiPc) was then encapsulated into the cup-shaped cavity of β -CD of the designed system, where F-couSiPc facilitated the oxidation of Ru(Bpy)₃²⁺ and achieved signal amplification. The antibody was labeled with MIL-125(Ti): Ru(Bpy)₃²⁺ and F-couSiPc. The ECL intensity gradually decreased with the increase in the DON concentration owing to the competitive binding reaction with the labeled antibody between the antigen immobilized on the electrode and free antigen, and the LOD was 0.03 pg/mL (S/N = 3). No changes in ECL response were found after the mixture of zearalenone, prostate specific antigen, aflatoxin B1, ochratoxin A and fumonisin was added to the solution (Fig. 3).[29]

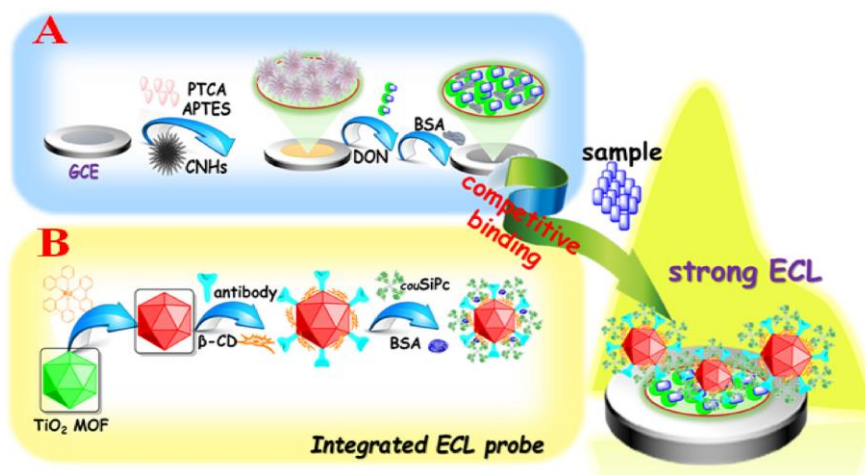


Figure 3. Fabrication process of the competitive-type ECL immunosensor.[29] Copyright 2018 Elsevier.

The sandwich method was commonly used to detect macromolecular antigens. Although different MOF materials were used in sandwich-type ECL immunosensors, $\text{Ru}(\text{Bpy})_3^{2+}$ was usually encapsulated in MOFs as a substrate to load sufficient antibodies (Ab_1) and provide high and jarless ECL signals. Secondary antibodies (Ab_2) were labeled with materials to quench the signal. Procalcitonin is a parameter for the diagnosis and monitoring of bacterial inflammatory diseases and infections.[30] Wang et al. designed mesoporous and hollow MIL-101(Al) to load $\text{Ru}(\text{Bpy})_3^{2+}$ with an amine-rich polymer polyethyleneimine (PEI) so as to acquire ECL initial signals that are stable and strong. Au nanoparticles (NPs) were immobilized on MIL-101(Al) to improve conductivity. *Via* the Au–NH₂ bond, Ab_1 was assembled on the electrode. $\text{Fe}_3\text{O}_4@\text{PDA}-\text{Cu}_x\text{O}-\text{Ab}_2$ as the quenching probe was prepared tactfully. The excited states of $\text{Ru}(\text{Bpy})_3^{2+}$ were quenched by the catechol or benzoquinone units in PDA and Cu^{2+} adsorbed by PDA *via* resonance energy transfer and electron transfer. In a wide range from 0.5 pg mL^{-1} to 100 ng mL^{-1} , the ECL immunosensor exhibited good linear relationship with a low LOD of 0.18 pg mL^{-1} ($\text{S/N}=3$). The carcinoembryonic antigen, immunoglobulin, prostate-specific antigen, and C-reactive protein had almost no quenching effect on the ECL signals, confirming that the designed electrochemical immunosensor had good selectivity (Fig. 4).[31] Similarly, a sandwich immunoassay for electrochemical luminescence detection of aminoterminal pro-brain natriuretic peptides (NT-proBNP) *via* the UiO-66-NH₂ carrier[32] and the ECL immunosensor for detecting Alzheimer's disease marker β -amyloid ($\text{A}\beta$) were successfully developed by Dong [33] and Zhao.[34], respectively.

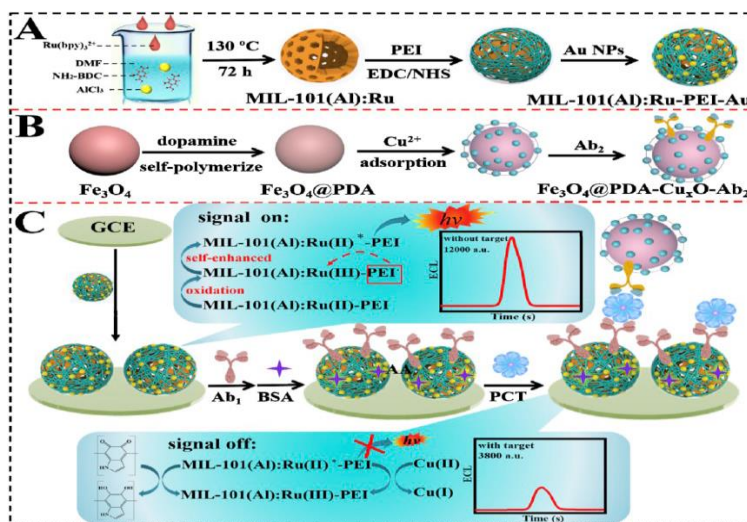


Figure 4. Schematic diagrams for (A) the synthesis steps of MIL-101(Al): Ru-PEI-Au and (B) Fe₃O₄@PDA-Cu_xO-Ab₂; (C) the fabrication process of the PCT sensor and the possible luminescence mechanism.[31] Copyright 2019 Elsevier.

$\text{Ru}(\text{bpy})_2(\text{mcpbpy})^{2+}$ is a derivative of $\text{Ru}(\text{Bpy})_3^{2+}$, which also has good luminous efficiency. Hu et al. prepared Ru-PCN-777 by coordinating $\text{Ru}(\text{bpy})_2(\text{mcpbpy})^{2+}$ with the Zr₆ nodes in MOF PCN-777 through strong binding between $-\text{COO}^-$ and Zr^{4+} . [35] A stable initial ECL signal was thus obtained. The use of enzyme-assisted DNA cycling amplification strategy further enhanced the ECL signal. As the concentration of Mucin 1 (MUC1), a transmembrane protein related to various types of cancer, [36] increased, the electrochemical luminescence signal gradually increased. The detection range of this ECL immunosensor for MUC1 was 100–100 ng/mL with the minimum LOD calculated to be 33.3 fg/mL (S/N = 3) (Fig. 5). The MOF material was replaced with Hf metal organic layer (HF-MOL) as a carrier, where MOL was also called MOF nanosheet. 2D MOLs could shorten the ion/electron transmission length and further improve the luminous effect. The electrochemical immunosensor prepared using PEI@Ru-Hf-MOL had a wider detection range and lower LOD for MUC1 with a good linear relationship obtained in the range of 1–10 ng/mL. The LOD was 0.48 fg/mL (S/N = 3). The addition of α -1-fetoprotein, β 2-microglobulin, cholesterol, and uric acid did not cause an obvious effect on the ECL signal of the immunosensor. [37]

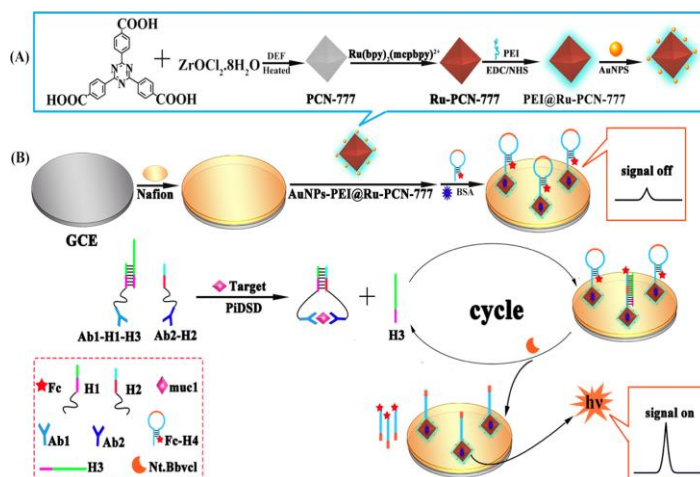


Figure 5. Fabrication of the immunosensor for the detection of MUC1.[35] Copyright 2019 American chemical society.

$\text{Ru}(\text{Bpy})_3^{2+}$ derivatives can also be used as organic ligands for MOFs. Tris(4,4'-dicarboxylic acid-2,2'-bipyridyl) ruthenium (II) $\text{Ru}(\text{dcbpy})_3^{2+}$ has six carboxyl groups that can coordinate to Zn^{2+} . Yan et al. synthesized a 2D Ru-MOF nanosheet using Zn^{2+} and $\text{Ru}(\text{dcbpy})_3^{2+}$. A novel luminescence-functionalized two-dimensional (2D) Ru-MOF nanosheet was labeled with cardiac troponin I (CTnI) Ab₂ by the sandwich method. The ECL signal of Ru-MOF nanosheets increased with the increase in the CTnI concentration. It turned out that the immunosensor had excellent sensitivity and high selectivity for CTnI in the range of 1–10 ng/mL with an LOD of 0.48 fg/mL (S/N = 3). Interfering proteins such as cardiac troponin, horseradish peroxidase, and human serum proteins were selected to assess the selectivity of this ECL immunosensor (Fig. 6), where high selectivity was achieved. [38] Based on the same mechanism, Xiong et al. constructed an ECL immunosensor to detect NT-proBNP using the luminescence-functionalized MOFs by Zn^{2+} and $\text{Ru}(\text{dcbpy})_3^{2+}$. [39]

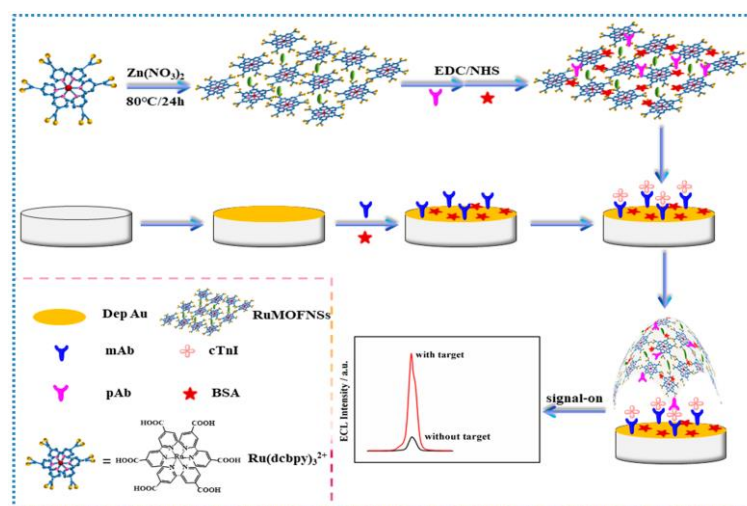


Figure 6. Fabrication process of the ECL immunosensor.[38] Copyright 2019 American chemical society.

Except for $\text{Ru}(\text{Bpy})_3^{2+}$ and its derivatives, luminol, *N*-(aminobutyl)-*N*-(ethylisoluminol) (ABEI), a special analogue, has gradually attracted peoples' interest as an ECL luminophor.[40] ABEI can react with reactive oxygen species (ROS), like superoxide anion radical (O_2^-) and hydroxyl radical (OH^-), to improve luminous efficiency. For example, Wang et al. prepared Co-MOFs/ABEI, an ideal nanocarrier, for enriching ABEI.[41] Co-MOFs have peroxidase-like activity, catalyze H_2O_2 decomposition, and further improve the ECL signal of ABEI. As the concentration of $\text{A}\beta_{42}$ labeled with Co-MOFs/ABEI increased from 10 fg/mL to 100 ng/mL, the electro luminescence intensity increased correspondingly, and the lower LOD was as low as 3 fg mL^{-1} ($\text{S/N} = 3$). The presence of four possible interfering substances, such as prostate-specific antigen, carcinoembryonic antigen, $\text{A}\beta_{40}$ and carbohydrate antigen 125, proved the good selectivity of the immunosensor (Fig. 7).[42]

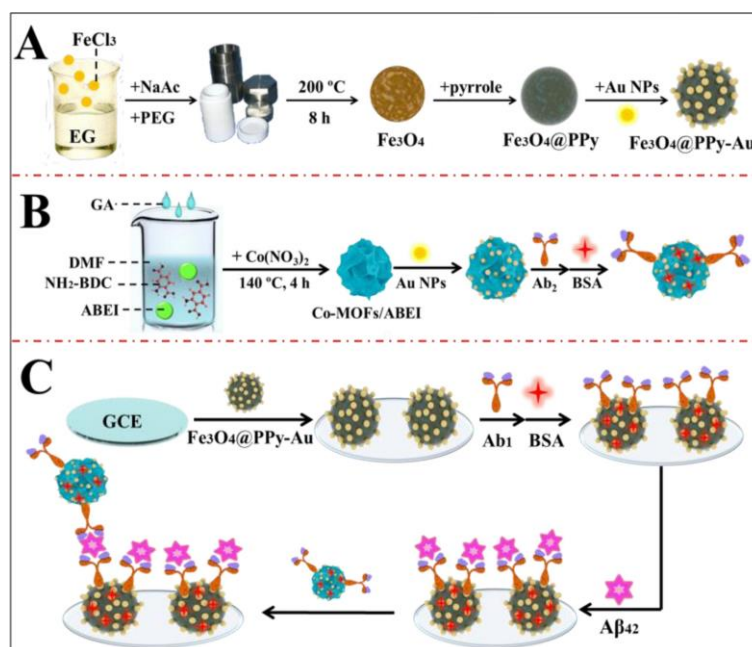


Figure 7. Preparation processes of (A) $\text{Fe}_3\text{O}_4@PPy\text{-Au}$, (B) Co-MOFs/ABEI-Au and (C) the $\text{A}\beta_{42}$ immunosensor.[42] Copyright 2019 Elsevier.

The aforementioned ECL immunoassays represented used a label, but can also be label-free. The graphene oxide (GO) nanosheets have various functional groups of carbonyl group, hydroxyl, epoxide, and carboxyl groups and excellent electrical conductivity. Based on the *in situ* self-assembly of Zn^{2+} and aminoalcohols triethanolamine (TEOA) on the surface of GO nanosheets, Qin et al. prepared GO-TEOA@MOF nanomaterials by adding $\text{Ru}(\text{Bpy})_3^{2+}$ to the solution for detection, where GO served as a co-reactant $\text{Ru}(\text{Bpy})_3^{2+}$ of ECL, producing a synergistic effect to enhance the electrochemical signal. The ECL immunosensor fabricated with GO-TEOA@MOFS was successfully used to determine human copeptin, achieving a linear concentration range from 5 pg/mL to 500 ng/mL and an LOD of 360 fg/mL. Glucose oxidase, cardiac troponin I, fatty acid-binding protein, L-cysteine, immunoglobulin G, and dopamine verified the high selectivity of the ECL immunosensor toward human copeptin (Fig. 8).[43]

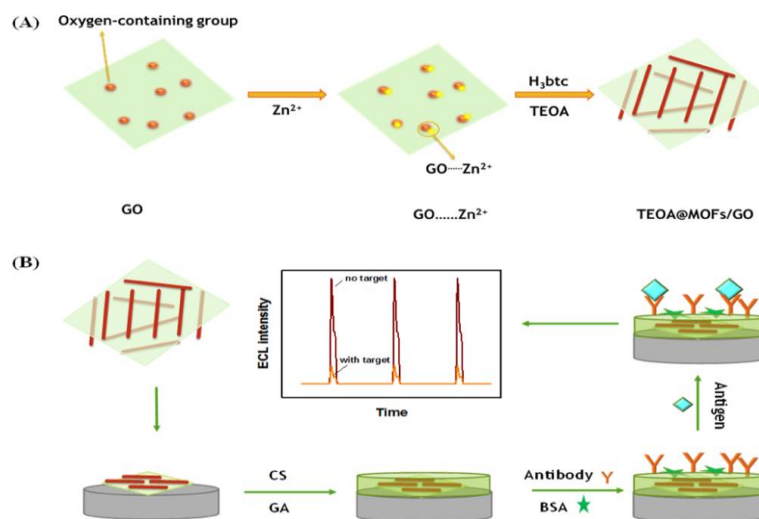


Figure 8. (A) TEOA functional MOF on GO nanosheets GO-TEOA@MOFs and (B) the establishment of the immunoassay system.[43] Copyright 2019 American chemical society.

CdSe quantum dots are known to have high ECL activity and sensing selectivity. MIL101(Cr) can adsorb and efficiently accumulate CdSe to amplify the ECL signal. The prepared CdSe quantum dot functional MOF (MIL-101-CdSe) has been considered as a label-free ECL immunosensor to achieve highly selective detection of carcino-embryonic antigen (CEA).[44]

The 4f orbitals exist in the electronic configuration of rare earth element atoms, and hence these atoms emit light of different wavelengths when 4f electrons radiate from a high energy level to a low energy level. Accordingly, rare earth elements can be used as metal centers to prepare luminescent metal-organic framework (LMOF) materials. Using Ce (III) as the metal nodes and 4,4',4'',4'''-(porphine-5,10,15,20-tetrayl)tetrakis(benzoic acid) (TCPP) as the co-linker, Zhou 0. successfully constructed a new type of LMOF structure and prepared an ECL immunosensor based on this LMOF to achieve the quantitative detection of proprotein convertase subtilisin/kexin type 9, a novel therapeutic target for dyslipidemia and atherosclerosis.[45] Polyamideamine dendrimers (PAMAM) and gold NPs have good electrical conductivity, which is conducive to enhancing the ECL signal. The newly designed ECL immunosensor showed desirable performance for PCSK9 analysis within a detection range from 50 fg/mL to 10 ng/mL and a low LOD of 19.12 ± 2.69 fg/mL. No obvious effect was found from the interfering substances of glucose, bovine serum albumin, dopamine, and L-cysteine on PCSK9 detection (Fig. 9).[46] Although the ECL immunosensors with a label showed higher sensitivity, the detection steps were simpler through the label-free ECL immunosensors. However, the LMOF-based label-free ECL immunosensors still have space for development in the future.

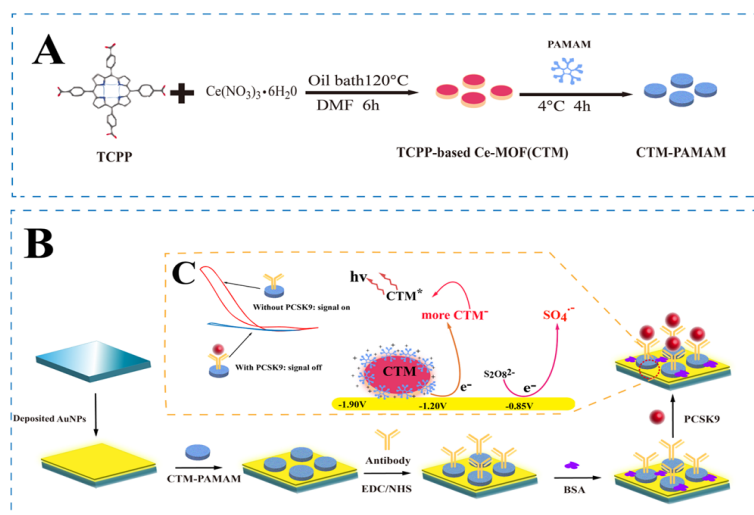


Figure 9. Schematic illustration of (A) the preparation process of Ce-TCPP-LMOF (CTM) and CTM-PAMAM and (B) ECL immunosensor fabrication. (C) Possible mechanism of the CTM-PAMAM/ $\text{S}_2\text{O}_8^{2-}$ /AuNP-GCE system.[46] Copyright 2020 American chemical society.

2.2 Detection of differential pulse voltammetry

The DPV method is a derivative method of linear scanning voltammetry and step scanning voltammetry by adding a certain voltage pulse on top of it. DPV is a linear scanning voltammetry method with a series of regular voltage pulses applied. The basic principle is to start from the base potential and then gradually increase from the initial voltage to the final voltage. During the application of the potential pulse (ΔE), the current is measured immediately before and after each potential pulse (τ), while simultaneously extracting the current difference as an output signal. The current is measured before the potential changes, and hence the influence of the charging current is reduced in this way while achieving higher sensitivity. It also saves time compared with other electrochemical analysis techniques such as EIS.[47]

If ions are present in the solution, the current is formed by the directed movement of electrons and ions. In DPV detection, MOFs with good electrical activity, such as Cu-MOFs, Zn-MOFs, and Fe-MOFs, are usually used. If necessary, Au NPs can be modified to enhance electrical signals further. The excellent conductivity of electroactive MOFs can be used not only as a carrier for labeled antibodies but also as a substrate on the electrode-fixed antibodies for label-free electrochemical immunosensors. The following two examples are label and label-free electrochemical immunosensors detected by the DPV method.

C-reaction protein (CRP) is an acute-phase protein with a positive pentamer structure. It has good stability and accuracy, and is a nonspecific marker of inflammation and tissue damage.[48] Based on the sandwich method, Liu et al. used platinum NP-modified covalent organic frameworks (Pt-COFS) with high electronic conductivity as substrates to capture CRP antibodies (Ab_1). CRP antibodies (Ab_2) were coupled to Au-MOFs *via* precious metal NPs and labeled with Au-MOFs. The MOFs were synthesized by dissolving 1,3,5-benzenetricarboxylic acid in a mixed solvent of methanol/water and then reacting with $\text{CuSO}_4 \cdot 7\text{H}_2\text{O}$. Au-MOF contains a large amount of Cu^{2+} and thus has a high electrochemical signal.

With the increase in the CRP concentration in the solution, the peak current intensity measured by the DPV method gradually increased with a low LOD of 0.2 ng/mL ($S/N = 3$). Carcinoembryonic antigen, human chorionic gonadotrophin, and glycine did not interfere with the detection of CRP using the prepared immunosensor, which was indicative of the high selectivity toward CRP detection (Fig. 10).[49]

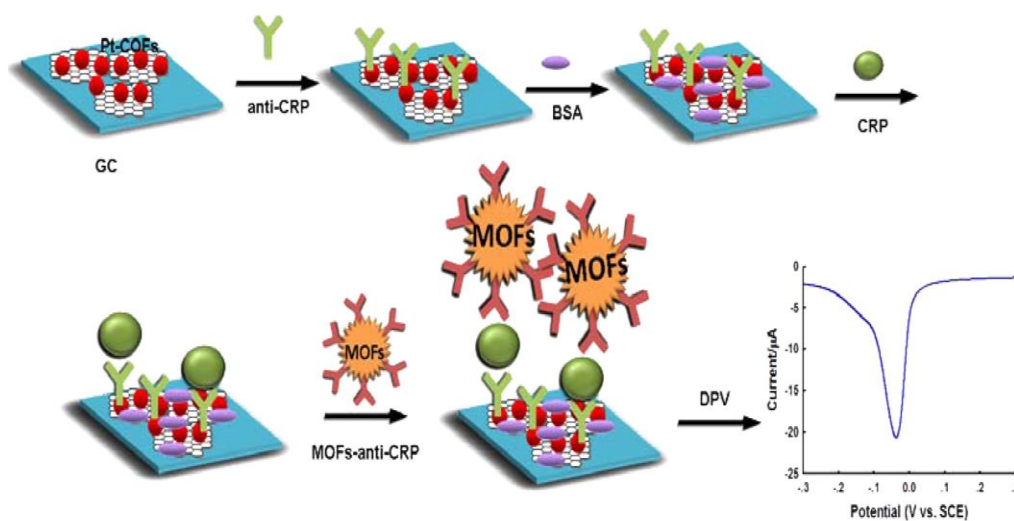


Figure 10. Schematic illustration of the electrochemical immunosensor.[49] Copyright 2016 American chemical society.

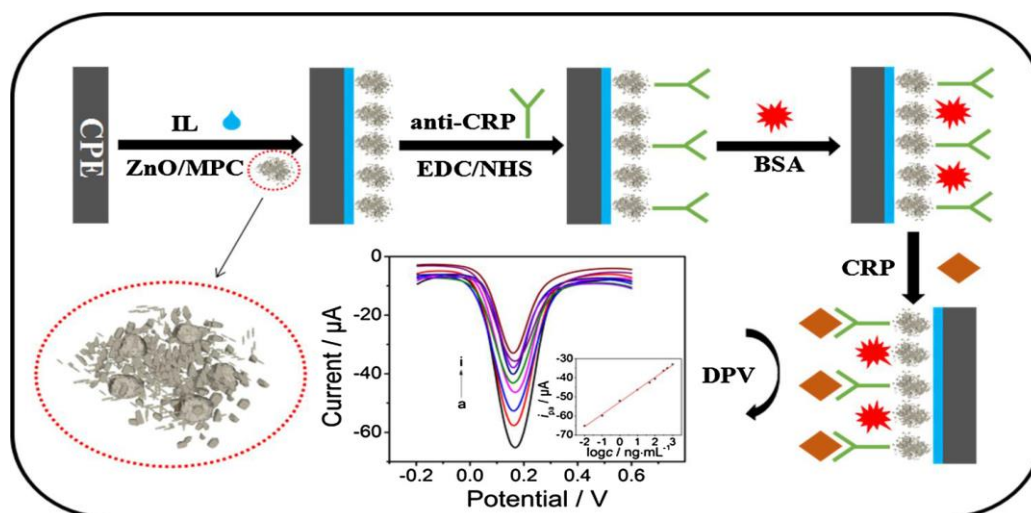


Figure 11. Schematic illustration of the process to prepare a CRP immunosensor.[50] Copyright 2019 Elsevier.

For detecting CRP, Dong et al. synthesized MOF materials of Zn-BDC-TED (white powder) using terephthalic acid (H_2BDC), triethylenediamine (TED), and $Zn(NO_3)_2 \cdot 6H_2O$, and obtained ZnO/MPC (black powder) through the thermolysis of Zn-BDC-TED ($500^\circ C$, 2 h) in the N_2 stream (Fig. 6). In this way, not only ZnO/MPC solved the characteristics of ZnO semiconductivity, but also MOF

materials could capture more anti-CRP. Using Zn-BDC-TED as a capturing probe, a label-free electrochemical immunosensor was prepared to analyze CRP. The peak current response of the immunosensor decreased with the increase in the CRP concentration, indicating that the immune complex generated on the electrode surface increased and blocked the electron transfer. The LOD was calculated to be 5.0 pg/mL ($S/N = 3$). Some effect was caused by adding interfering substances, such as immunoglobulin G, BSA, glucose, uric acid and ascorbic acid, into the standard samples for the detection of CRP (Fig. 11), revealing the excellent selectivity of the Zn-BDC-TED-based electrochemical immunosensor.[50]

For the other label or label-free electrochemical immunosensors based on the DPV method, we only listed them in Table 1, because MOFs played a similar role in these electrochemical immunosensors.[50]

2.3 Detection of Square Wave Voltammetry

For SWV, the baseline potential gradually swept from the initial potential to the termination potential in a step form. A square wave voltage was superimposed, and the basic voltage increased after each square wave cycle. Current sampling was performed at the end of the forward and reverse steps, and the difference between the two sampled currents was plotted against the voltage. Generally, as the enrichment time increased, the adsorption amount of the analyte on the electrode increased, and the corresponding redox peak current increased. SWV could more effectively suppress the background current, with higher sensitivity and faster scan rate compared with DPV.[51]

Amyloid is one of the main diagnostic biomarkers and therapeutic targets for Alzheimer's disease with the most obvious symptoms of memory loss, abnormal brain nerve formation, and severe brain damage.[52] Han et al. improved ferrocene as a signal probe exposed on the solid outer surface. Although the use of ferrocene redox to make electrochemical immunosensors has long been applied, pure ferrocene is difficult to be immobilized on the electrode surface (Fig. 9) so that the electrode surface cannot achieve fast signal transmission. A flower-like ferrocene (Fc) Fc-Zn-MOF was obtained by the covalent bonding of Fc and Zn-MOF, in which a high amount of Fc signal units was periodically arranged in a transparent porous structure. The MOF framework prevented the leakage of signal molecules and improved stability. A sandwich immune response between Au/Fc-Zn- β and Ab₂ labeled with Au/Fc-Zn-MOF ensured specificity and a better electrochemical signal output. The SWV method proved the good linear range of the sensor as 0.0001–100 ng/mL, a low LOD of 0.03/pg/mL, good sensitivity, and high selectivity (Fig. 12).[53]

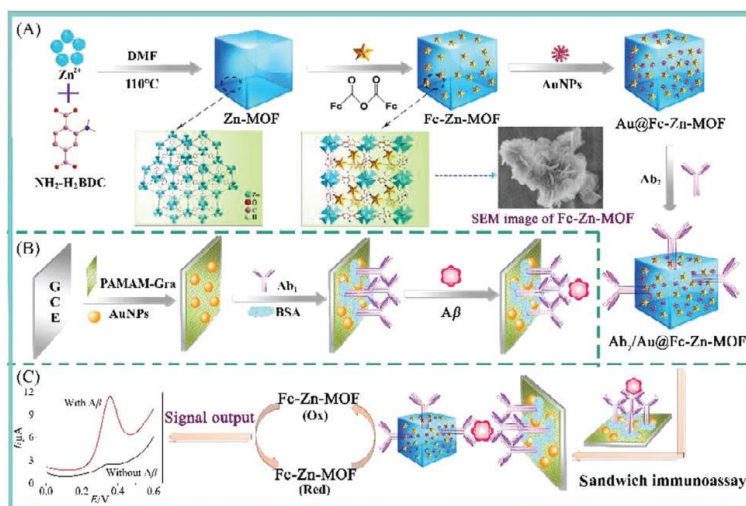


Figure 12. Illustration of the preparation processes of (A) $Ab_2/Au@Fc-Zn-MOF$ (Ab_2 bioconjugate) fabrication, (B) electrochemical immunosensor, and (C) sandwich immunoassay for Ab detection.[53] Copyright 2017 Royal Society of Chemistry.

Similarly, an electrochemical immunosensor using SWV was prepared using the enzyme-like activity of MOFs. We could coat the surface of the electrode with a redox-active conductive substance and record the change in the electrochemical signal when the antigen–antibody immune reaction occurred. Feng's group produced Fe-MOF and Fe-MOF surface-loaded Au NP-linked labeled antibody (Ab_2) (Fig. 10). Besides the reduced GO-Au NPs nanocomposite coated with Ab_1 on the electrode surface, a thin layer of methylene blue (MB) was also formed. The antigen–antibody specific binding and Fe-MOF could catalyze H_2O_2 to produce $\cdot OH$, and degrade MB, and hence Au-rGO increased the surface electron transfer of the electrode. Based on these advantages, the SWV method can be used to achieve ultra-sensitive detection of prostate-specific antigen (PSA). It has a lower LOD of 0.13 pg/mL ($S/N = 3$) and a wide analytical range from 0.001 to 100 ng/mL. Bovine serum albumin, glutamic acid, uric acid, immunoglobulin, serum creatine, and creatine kinase-19 did not cause large current fluctuations, fully demonstrating that the specificity of the immunosensor is good (Fig. 13).[54] Dong constructed Fe^{2+}/Fe^{3+} -MOF with fully dispersed metal sites, which significantly improved the atomic utilization and mass transfer rate and exhibited better electrochemical performance. Based on the electrochemical behavior, the catalytic cycle mechanism and electron transfer routes between MoS_2 and Fe^{2+}/Fe^{3+} -MOF were further discussed.[55]

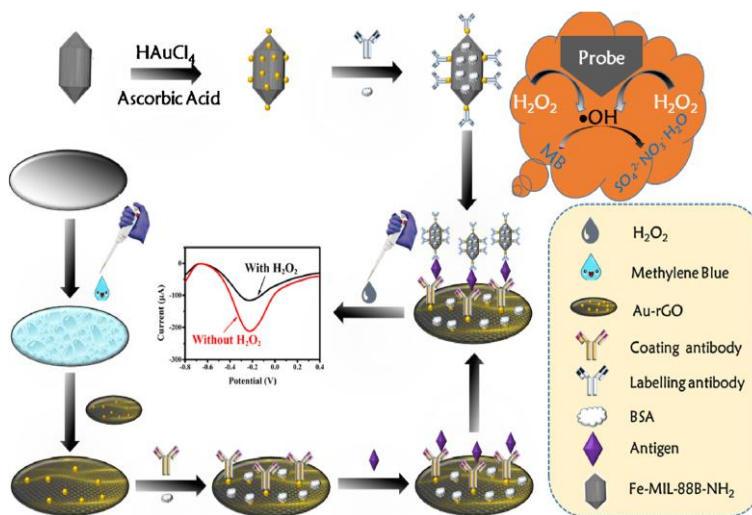


Figure 13. Construction steps and mechanism of an immunosensor.[54] Copyright 2021 Springer nature.

Both the DPV and SWV detection methods are based on the improvements in cyclic voltammetry to reduce the background current. When the detection methods are DPV and SWV, MOFs with good electrical activity are often selected to construct sandwich immunosensors. Chen et al. prepared a label-free electrochemical immunosensor based on Cu-MOF nanowires to detect PSA. Cu(II)1,4-naphthalenedicarboxylic acid (1,4-NDC) nanowires contain many uncoordinated carboxyl groups and can bind to the amino groups of PSA antibodies. An immune response occurs, and the electrical signal is reduced due to the electrical insulation of the PSA antigen. The LOD of this immunosensor was as low as 4.4 fg/mL ($S/N = 3$), and a good linear relationship was obtained in a wide linear range from 0.1 pg/mL to 20 ng/mL. On adding serine, human chorionic gonadotropin, and alpha-fetoprotein, the DPV signal changed by less than 6%, which proved the good detection performance of the Cu-MOF-based electrochemical immunosensor (Fig. 14).[56]

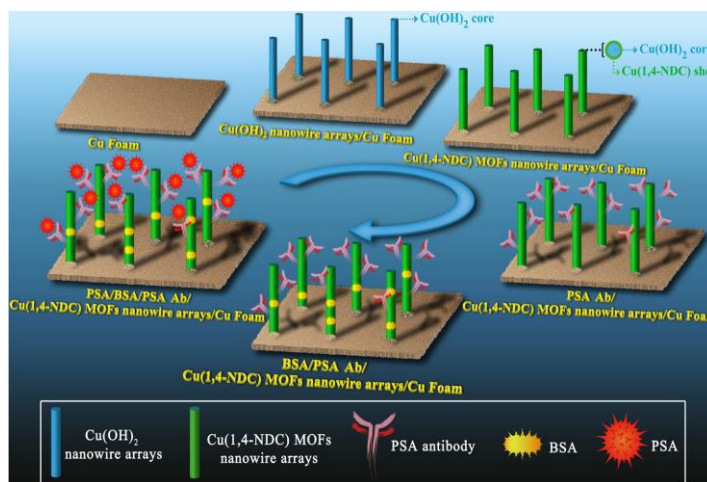


Figure 14. Preparation of an electrochemical immunosensor for PSA detection .[56] Copyright 2021 Springer nature.

2.4 Detection of Electrochemical Impedance Spectroscopy

An electrochemical impedance immunosensor measures the target according to the changing impedance value of the electrode surface caused by the specific binding or reaction of the immune complex or enzyme on the electrode surface. By controlling the alternating current (AC) potential of the electrode or the AC current of the electrode based on a small-amplitude sine wave (usually less than 10 mV), the sine wave AC impedance of the electrode is measured and the electrochemical parameters of the electrode are calculated. The impedance value can be obtained directly from the AC impedance spectrum. The characteristics of AC impedance technology are as follows: it has the high-precision experimental ability; it can obtain the average value for a long time; and the interference of the small-amplitude signal on the battery makes the electrode reaction in a state close to equilibrium, which greatly simplifies the kinetics and diffusion process. EIS-based measurement over a wide frequency range can be used to study the changes in electrochemical reactions and electrode interfaces.[57]

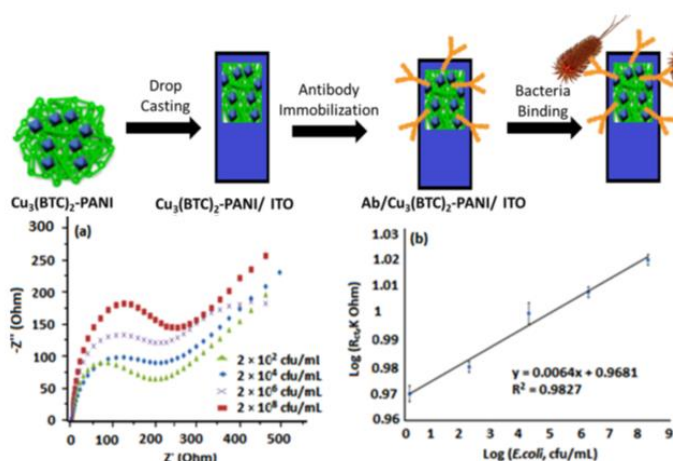


Figure 15. Schematic fabrication of bioelectrode and its subsequent utilization for the EIS sensing of *E. coli*. (a) EIS of the fabricated immunosensor [Ab/ $\text{Cu}_3(\text{BTC})_2\text{-PANI/ITO}$] toward different concentrations of *E. coli*. (b) Calibration curve of the developed Ab/ $\text{Cu}_3(\text{BTC})_2\text{-PANI/ITO}$ (variation in the values of charge transfer resistance versus the number of bacterial colonies analyzed).[61] Copyright 2019 Elsevier.

Previously, ($\text{Cu}_3(\text{BTC})_2$, BTC^{3-} (1,3,5-benzenetricarboxylate), also known as HKUST-1 or MOF-199, (BTC: 1,3,5-benzenetricarboxylic acid), has been reported for diverse applications, such as gas storage [58], catalysis [59], and sensing of analytes [60] (methanol, ethanol, propanol, and nitric oxide). Arushi et al. prepared a uniform composite film by mixing $\text{Cu}_3(\text{BTC})_2$ with polyaniline (PANI) (Fig. 4). PANI, as a kind of polymer compound, has special electrical and optical properties and can have conductivity and electrochemical properties after doping. The obtained $\text{Cu}_3(\text{BTC})_2/\text{PANI}$ film combined the excellent electrochemical properties of PANI and the large specific surface area of $\text{Cu}_3(\text{BTC})_2$, and thus showed high pore volume and high thermal stability. The thin-film electrode is connected to an *Escherichia coli* (*E. coli*) anti-*E. coli* antibody (Ab) to form an Ab/ $\text{Cu}_3(\text{BTC})_2/\text{PANI}$

sensor based on an immune response for detecting *E. coli* in an actual water sample with high sensitivity. The LOD of the proposed sensor was calculated to be 2 CFU/mL ($S/N = 3$). Good specificity was not affected in the presence of nonspecific bacteria (*Staphylococcus aureus*), indicating its good specificity (Fig. 15).[61]

Besides serving as a carrier for antibodies, Cu-MOFs can also play an enzyme-like catalytic role. Zhang's group designed a Cu-MOF electrochemical immunosensor based on a catalytic free radical cascade to detect CA15-3, one of the biomarkers of breast cancer, the content of which was below 30 U/mL in healthy human serum.[62] Cu-MOF bound to the CA15-3 antibody (Ab_2), and glucose oxidase (GOx) as an immunoprobe. The antibody (Ab_1) was incubated overnight on the electrode surface, and the bovine serum albumin (BSA) was used to block the nonspecific binding sites. Ab_2 is a Cu-MOF-labeled specific antibody that also binds to the surface of the carrier *via* the antigen. GOx can catalyze the conversion of glucose into hydrogen peroxide in blood samples, which reacts with acetylacetone (ACAC) under the action of Cu-MOF to generate ACAC radicals for the polymerization of N-isopropylacrylamide (NIPAM). Free radical polymerization produces the polymer poly-N-isopropylacrylamide (PNIPAM), and its conductivity hinders the charge transfer of $[Fe(CN)_6]^{3-/4-}$, increasing the resistance difference significantly. The content of CA15-3 in the blood can be calculated by EIS based on this detection principle with an LOD of 5.06 μ M/mL ($S/N = 3$). The difference in the charge transfer resistance (R_{ct}) value after adding CA12-5, CA9-9, CA24-2, and CEA in the mixture with CA15-3 only was negligible, proving the good specificity of the electrochemical immunosensor (Fig. 16).[63]

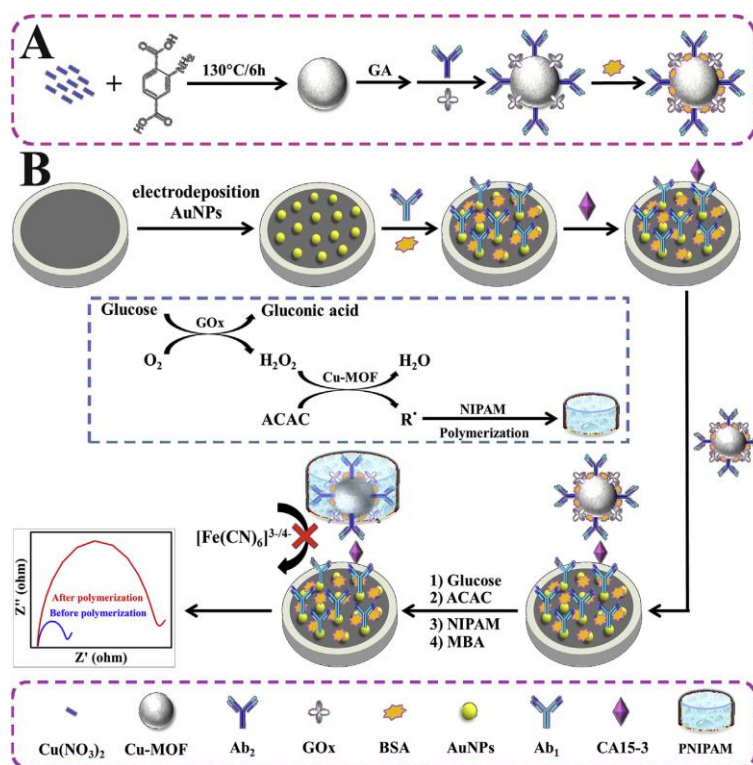


Figure 16. Schematic illustration of the preparation process of immunoprobes (A); cascadecatalysis-initiated radical polymerization triggered signal amplification for the electrochemical detection of CA15-3 (B).[63] Copyright 2019 Elsevier.

Liu designed aluminum-based MOFs, 516-MOFs. The presence of the organic elements in 516-MOFs reduced the electrochemical performance. A high antibody-loading capacity of 516-MOF and the immune reaction successfully captured vomitoxins. The adsorption of antibodies and the detection of albuterol prevented the electron transfer between the electrode surface and the electrolyte solution. The impedance signal increased significantly to achieve the purpose of detection.[64] Using CeFe-MOF, Wang et al. prepared a series of bimetallic cerium and iron oxide NPs embedded in a mesoporous carbon matrix (CeO₂/FeO_x/MC) through different high-temperature roasting to achieve countermeasures for the selective detection of CA19-9. Antibody molecules could be adsorbed on CeO₂ through antibody carboxyl groups, and Fe₂O₃ improved electrochemical performance. Moreover, the graphitized carbon layer with a porous structure and high specific surface area was also used as the matrix to provide abundant interface positions for antibody immobilization.[65]

In electrochemical impedance immunoassays, a detectable signal from a direct reaction between an antigen and an antibody is often insufficient. The use of MOF materials for easy modification and high carrier capacity combined with antibodies is promising for preparing electrochemical immunosensors.

2.5 Detection of amperometry

The amperometric method is used at a fixed or variable electrode potential (usually a fixed applied potential). The current generated by the reaction of the analyte on the electrode is measured as a sensor signal. Using a constant-voltage *i-t* curve, the response current signal is recorded with the change in the analyte concentration. The key of the amperometric method is the response intensity and response time of the current signal.[66] The high specific surface area of the MOF material can avoid the nonspecific adsorption of the antigen and inactivation of the enzyme.

Microcystin-LR (MC-LR) is the most serious cyanotoxin to fresh water. Zhang et al. used high-conductivity GO as a matrix to immobilize MC-LR antibodies. Au NPs were loaded on MIL-101(Cr) to form the Au NPs@MIL-101 composite, and the composite-labeled BSA-MC-LR and MC-LR competed with the anti-MC-LR immobilized on the electrode surface. The Au NPs@MIL-101 composite can catalyze the oxidation of ascorbic acid and generate a response current signal inversely proportional to the concentration of MC-LR, enabling the quantitative detection of MC-LR. The electrochemical immunosensor displayed a good linear relationship in the range of 0.05–75 mg/mL and a low LOD of 0.02 ng/mL (S/N = 3). The addition of the MC-YR and MC-RR did not cause interference to the detection of MC-LR, showing the high selectivity of the proposed Au NPs@MIL-101-based immunosensor toward MC-LR (Fig. 17).[67]

Maduramicin (MD) is an antibiotic commonly used in animal feed additives. Its incorrect use may pose a potential risk of coronary artery dilation in humans.[68] Hu et al. fixed the antigen MD-BSA with Au NPs. Hemin was encapsulated into MIL-88(Fe) and then further modified with AuPt NPs. This prepared composite also had horseradish peroxidase (HRP)-coupling affinity and served as a carrier of pure goat anti-mouse antibody (Ab₂-HRP). The labeled hemin@MIL-88/AuPt-AB₂-HRP MD antibody competed with the free antibody for the antigen fixed on the electrode surface. Under the co-catalysis of

hemin, AuPt NPs, and HRP, the detection range of this new immunosensor was 0.1–50 ng/mL with the LOD as low as 0.045 ng/mL (S/N=3). Interfering substances such as dinitroformamide, nicaraguapazine, and sulfadiazine caused no significant signal change compared with the current in the blank group (Fig. 18).[69] The hollow nanobox-MOFs (HNMs) with tin dioxide–functionalized reduced GO (rGO-SnO₂) and the AuPt alloys encapsulated outside (rGO-SnO₂/HNMs/AuPt) was prepared as the matrix. The material had a unique structure, a large specific surface area, and good electrical activity, thereby achieving high sensitivity to detect the Lag-3 protein by the HNM/AuPt-based immunosensor.[70]

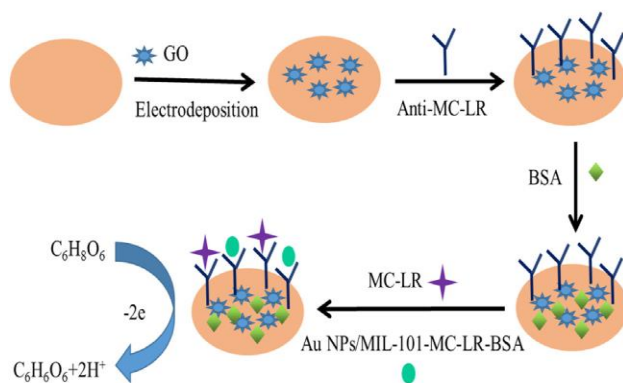


Figure 17. Preparation of the Au NPs@MIL-101-based immunosensor.[67] Copyright 2019 Elsevier.

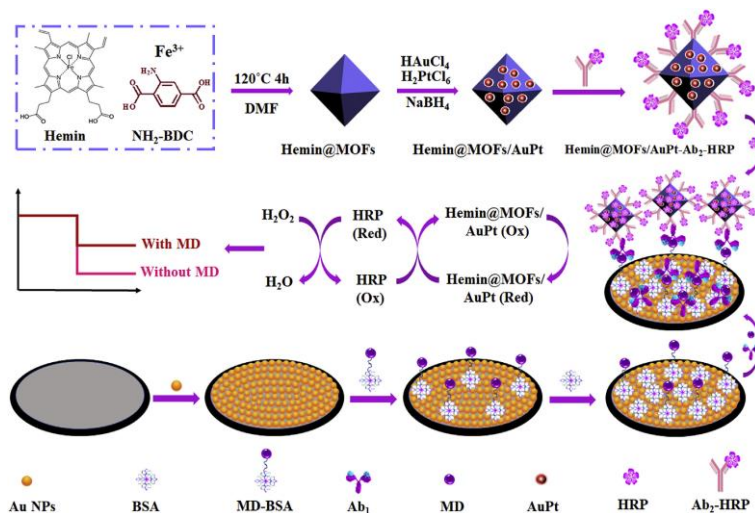


Figure 18. Preparation of hemin@MOFs/AuPt-Ab₂-HRP/HRP bioprobes and the proposed competitive electrochemical immunosensor.[69] Copyright 2019 Elsevier.

Li et al. designed a sandwich-type electrochemical immunosensor by encapsulating Ce-MOF with hyaluronic acid (HA), Ag NPs, and HRP-labeled anti-CEA antibody. The hydroxyl and carboxyl groups in HA facilitated Ce-MOF to modify more Ag NPs and HRP to catalyze the reduction of H₂O₂ for amplifying the current signal. The current signal had a good relationship with the logarithm of CEA concentration in the range of 1 pg/mL to 80 ng/mL, and the LOD was 0.2 pg/mL (Fig. 19).[71]

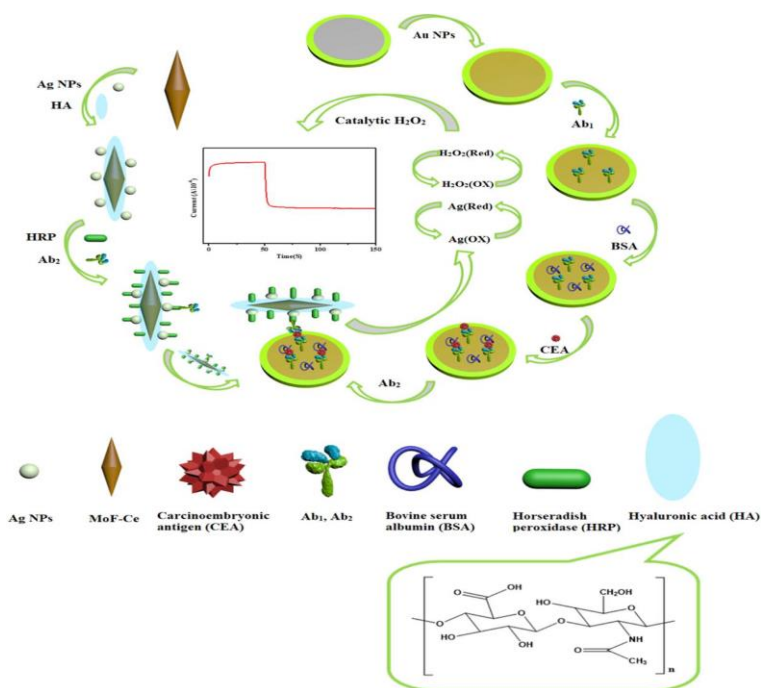


Figure 19. Layered self-assembly process of the Ce-MOF-based immunosensor.[71] Copyright 2020 Institute of Physics.

Dai constructed a sandwich-type Pd/NH₂-ZIF-67-based electrochemical immunosensor for PSA detection (Fig. 20). The Au-NH₂ bond formed by Au NPs fixed the Ab₁ on the electrode surface. Also, Pd NPs were supported on the electroactive NH₂-ZIF-67 *via* the Pd-NH₂ bond as a signal biomarker. A signal biomarker was connected with the Ab₂ *via* a Pd-H₂ bond where Pd played an enzyme-like catalytic role. Electroactive ZIF-67 could doubly fictionalize as a support for Pd NPs and a synergistic catalyst for the effective decomposition of H₂O₂. The amperometric method was used to measure the current response produced over the electrode surface to quantitatively determine PSA. Under the optimal conditions, the detection range of this immunosensor was 100 fg/mL to 50 ng/mL, with a low LOD of 0.03 pg/mL (S/N = 3). The good selectivity of this immunosensor was confirmed by the unchanged current signal after adding interference substances BSA, human immunoglobulin G, ascorbic acid, hepatitis B surface antigen, and glucose in human serum.[72]

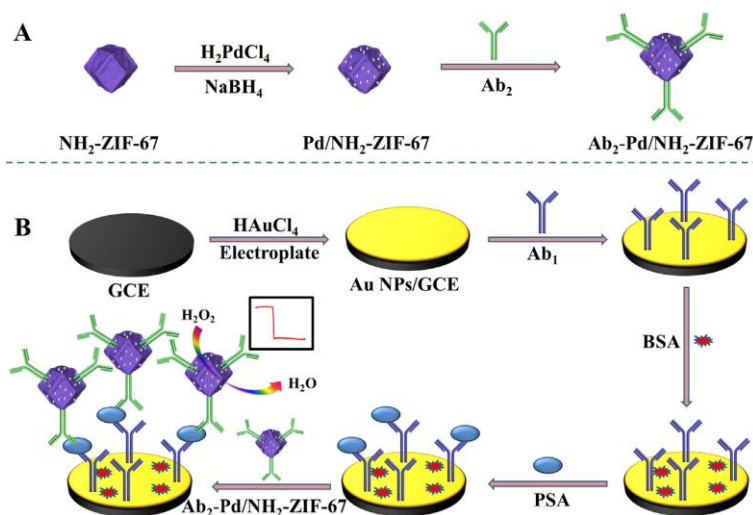


Figure 20. Preparation illustration of (A) Ab_2 -Pd/NH₂-ZIF-67 and (B) the immunosensor.[72] Copyright 2018 Elsevier.

Co-MOF has been used to immobilize ABEI molecules in electrochemical immunosensors detected by ECL, but Co-MOF nanowires as carriers have not been reported for constructing electrochemical sensors. The chrysanthemum-like Co-MOFs/CuAu nanocomposites could be used not only as electrode modification materials to immobilize antibodies but also as signal amplification material. Co-MOF could catalyze the oxidation of H₂O₂ as a function of HRP (Fig. 21). The current response was reduced to various degrees with more NMP-22 antigen (Ag) specifically attached to the immunosensor. The label-free immunosensor displayed a good linear relationship in the concentration range of 0.1 pg/mL to 1 ng/mL and a low LOD of 33 fg/mL (S/N = 3).[73]

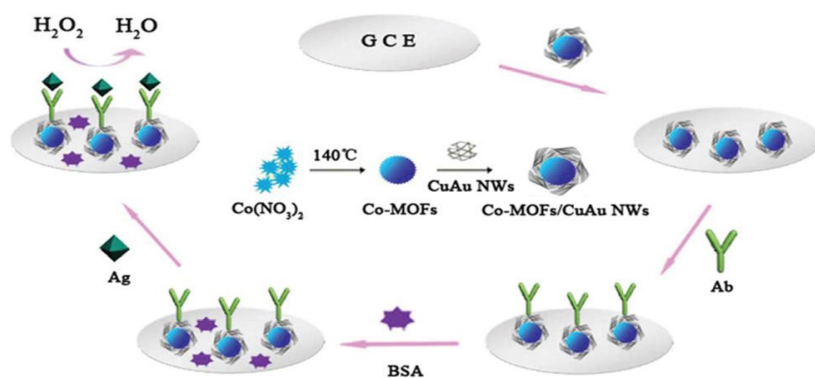


Figure 21. Schematic illustration to fabricate the proposed label-free electrochemical immunosensor.[73] Copyright 2019 Royal Society of Chemistry.

2.6 Detection of conductometry

Conductance is the inverse of resistance, while measuring conductance is essentially measuring resistance. Conductivity analysis is a method to determine the ion content by measuring the resistance

of the solution between two electrodes. Since the conductivity of a solution is not a characteristic parameter of an ion, but a common contribution of all ions in the solution, the selectivity of the conductivity analysis method is usually extremely poor. Although electroactive MOFs are used for the conductance sensing of gases, MOFs for the conductance sensing of biomolecules are still in their infancy.[74]

The surface modification of MOFs with silica coating can not only optimize their biofunctional conditions but also improve their water stability and dispersibility. Sanjeev et al. assembled SiO₂ on the conductive substrate of Cu₃(BTC)₂-doped PANI NH₂-BDC (NH₂-BDC:2-aminobenzene-1,4-dicarboxylic acid). The film showed good conductivity in the range of 35 μ A and was coupled with an anti-atrazine antibody to form a new type of immunosensing platform (Fig. 22). The film showed high sensitivity to the detection of pesticide atrazine (LOD = 0.01 nM) and strong specificity, with no effect caused by pesticides such as endosulfan, parathion, paraoxon, malathion, and monochromatic phosphorus on the target detection.[75] Tetracyanoquinodimethane (TCNQ) is a redox-active molecule, and its confinement in the porous network of MOFs can lead to the formation of a charge-transfer complex between Cu (II) and TCNQ. Sanjeev et al. increased the conductivity of the substrate by 9 orders of magnitude (from 10⁻¹² s to 10⁻³ s) through doping the Cu₃(Btc)₂ film with TCNQ. The conductive platform was modified with antibodies, and a PSA immunosensor was thus designed.[76]

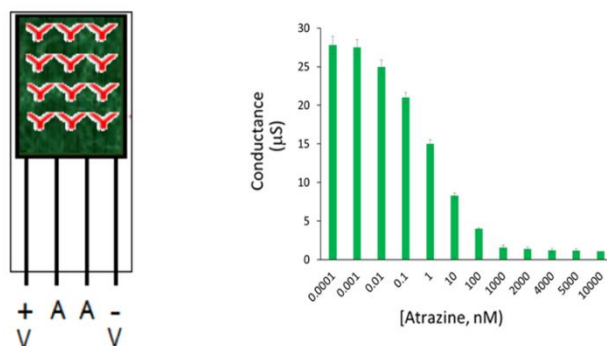


Figure 22. Conductometric immunosensing platform of Cu-MOFs.[76] Copyright 2017 Elsevier.

Table 1. Summary of the reported MOF-based electrochemical immunosensor

MOFs	Target	Linear range	LOD	Ref
Detection of ECL				
Ru(bpy) ₃ ²⁺ /UiO-67(Zr)	DES	10 ⁻⁵ –50 ng/mL	3.27 fg/mL	[27]
MIL-125(Ti)	DON	10 ⁻⁴ –20 ng/mL	0.03 pg/mL	[29]
MIL-101(Al)-NH ₂	PCT	5.0×10 ⁻⁴ –100 ng/mL	0.18 pg/mL	[31]
UiO-66(Zr)-NH ₂	NT-proBNP	10 ⁻⁶ –100 ng/mL	0.41 fg/mL	[32]
UiO-66(Zr)-NH ₂ and MIL-101(Cr)	A β	10 ⁻⁵ –50 ng/mL	3.32 fg/mL	[33]
Ru(bpy) ₃ ²⁺ /zinc oxalate and Au/NiFe	A β	10 ⁻⁴ –50 ng/mL	13.8 fg/mL	[34]
Ru-PCN-777(Zr)	MUC1	10 ⁻⁴ –100 ng/mL	33.3 fg/mL	[35]
PEI/Ru-Hf-MOL	MUC1	10 ⁻⁶ –10 ng/mL	0.48 fg/mL	[37]
RuMOFNSs	cTNI	10 ⁻⁶ –10 ng/mL	0.48 fg/mL	[38]
Zn ²⁺ / Ru(dcbpy) ₃ ²⁺	NT-proBNP	5.0×10 ⁻³ –25 ng/mL	1.67 pg/mL	[39]

ABEI/Co-MOFs	A β ₄₂	10 ⁻⁵ –100 ng/mL	3.00 fg/mL	[42]
GO-TEOA/MOF	copeptin	5.0×10 ⁻³ –500 ng/mL	360 fg/mL	[43]
MIL-101(Cr)-CdSe	CEA	10 ⁻⁶ –100 ng/mL	0.33 fg/mL	[44]
Ce-TCPP-LMOF	PCSK9	5.0×10 ⁻⁵ –10 ng/mL	19.12 ± 2.69 fg/mL	[46]
Detection of DPV				
Au-MOFs	CRP	1–400 ng/mL	0.2 ng/mL	[49]
Zn-BDC-TED	CRP	10 ⁻² –1000 ng/mL	5.00 pg/mL	[33]
Ag-MOFs	CEA	5.0×10 ⁻² –120/ng mL	8.00 fg/mL	[77]
AuNPs/Cu-TPA	CEA	10 ⁻¹ –80 ng/mL	0.03 ng/mL	[78]
Fe ₃ O ₄ /TMU-10(Ni)	PSA	10 ⁻³ –100 ng/mL	0.45 pg/mL	[79]
AuNPs/N-GNRs-Fe-MOFs	Gal-3	10 ⁻⁴ –50 ng/mL	33.33 fg/mL	[80]
CdS/ZIF-8(Zn)	E. coli O157:H7	10–10 ⁸ cfu/mL	3.00 cfu/mL	[81]
AuNPs-PtNPs-MOFs	NMP22	5.0×10 ⁻³ –20 ng/mL	1.70 pg/mL	[82]
Zn/Ni-ZIF-8(Zn)-800	Monensin	2.5×10 ⁻¹ –100 ng/mL	0.11 ng/mL	[83]
Detection of SWV				
Fc-Zn-MOF	A β	10 ⁻⁴ –100 ng/mL	0.03 pg/mL	[53]
AuNPs/Fe-MOF	PSA	10 ⁻³ –100 ng/mL	0.13 pg/mL	[54]
Cu-MOFs	PSA	10 ⁻⁴ –20 ng/mL	4.40 fg/mL	[56]
Detection of EIS				
Cu ₃ (BTC) ₂	E. coli	2.0–2.0×10 ⁸ cfu/mL	2.00 cfu/mL	[61]
Cu-MOF	CA15-3	10 ⁻² –10 mU/mL	5.06 μ U/mL	[63]
Al-MOF	vomitoxin	10 ⁻³ –0.5 ng/mL	0.70 pg/mL	[64]
CeFe-MOF	CA19-9	10 ⁻¹ –10 ⁴ mU/mL	10 μ U/mL	[65]
Detection of amperometry				
AuNPs/MIL-101(Cr)	MC-LR	5.0×10 ⁻⁵ –75 μ g/mL	0.02 ng/mL	[67]
Hemin/MIL-88(Fe)-NH ₂ /AuPt	MD	10 ⁻¹ –50 ng/mL	45.00 pg/mL	[69]
rGO-SnO ₂ /HNMs/AuPt	LAG-3	10 ⁻² –1000 ng/mL	1.10 pg/mL	[70]
HA/Ce-MOF/Ag-HRP	CEA	10 ⁻³ –80 ng/mL	0.20 pg/mL	[71]
Pd/NH ₂ -ZIF-67(Co)	PSA	10 ⁻⁴ –50 ng/mL	0.03 pg/mL	[72]
Co-MOFs/CuAu NWs	NMP-22	10 ⁻⁴ –1 ng/mL	33.00 fg/mL	[73]
Detection of conductometry				
Cu ₃ (BTC) ₂	atrazine		0.01 nM	[75]
TCNQ-Cu ₃ (BTC) ₂	PSA	0.1–100 ng/mL	0.06 ng/mL	[76]

3. CONCLUSION AND OUTLOOK

In this review, we first introduced the mechanism of antigen–antibody immune response in electrochemical sensors. According to the types of electrochemical detection methods, the different applications of MOFs in the preparation of MOF-based electrochemical immunosensors were discussed in detail and are summarized in Table 1. The introduction of antigens or antibodies into MOFs could greatly improve the selectivity of electrochemical immunosensors toward targeted proteins and bacteria. Compared with the simple labeling of free antibodies, MOFs, as immobilized carriers, could effectively increase the antibody load, and some MOFs played an enzyme-like catalytic role. However, the research in this area is still in its infancy, with still much room for improvement, as concluded below:

(1) When MOFs play an enzyme-like catalytic role, the related reaction mechanism and process can be further studied.

(2) Both Cu-MOFs and Ce-MOFs have good electrical activity and are widely used in electrochemical immunosensors. However, heavy metal ion-containing ligands (Pt and Bi) and magnetic MOF ligands (Fe and Ni) need to be developed and explored.

(3) The loading of multiple antibodies into MOF materials at the same time and the construction of electrochemical immunosensors for the simultaneous detection of multiple antigens should be investigated.

ACKNOWLEDGMENT

This study was financially supported by the Shanghai Natural Science Foundation (19ZR1434800 and 19ZR1461900) and Shanghai Collaborative Innovation Center of Energy Therapy for Tumors. The authors greatly appreciated this support.

References

1. G.B.o.D.C. Collaboration, *JAMA Oncology*, 4 (2018) 1553.
2. N.C. Cullen, A. Leuzy, S. Palmqvist, S. Janelidze, E. Stomrud, P. Pesini, L. Sarasa, J.A. Allué, N.K. Proctor, H. Zetterberg, J.L. Dage, K. Blennow, N. Mattsson-Carlgren, O. Hansson, *Nat. Aging*, 1 (2021) 114.
3. B. Jurado-Sánchez, *Biosens.*, 8 (2018).
4. C.A. Donini, M.K.L. Silva, G.R. Bronzato, A.L. Leão, I. Cesarino, *Journal of Solid State Electrochem.*, (2019) 2011.
5. J.J. Taylor, K.M. Jaedicke, R.C. van de Merwe, S.M. Bissett, N. Landsdowne, K.M. Whall, K. Pickering, V. Thornton, V. Lawson, H. Yatsuda, T. Kogai, D. Shah, D. Athey, P.M. Preshaw, *Sci.Rep.*, 9 (2019) 11034.
6. Z. Ye, G. Li, L. Xu, Q. Yu, X. Yue, Y. Wu, B. Ye, *Talanta*, 209 (2020) 120611.
7. J.e. Xiong, S. Li, Y. Li, Y. Chen, Y. Liu, J. Gan, J. Ju, Y. Xian, X. Xiong, *Chem. Res.Chin Univ.*, (2019) 787.
8. H. You, Z. Mu, M. Zhao, J. Zhou, Y. Yuan, L. Bai, *Sens. Actuators, B.*, 305 (2020) 127483.
9. R. Antiochia, *Biosens. Bioelectron.*, 173 (2021) 112777.
10. A. Quijano-Rubio, H.-W. Yeh, J. Park, H. Lee, R.A. Langan, S.E. Boyken, M.J. Lajoie, L. Cao, C.M. Chow, M.C. Miranda, J. Wi, H.J. Hong, L. Stewart, B.-H. Oh, D. Baker, *Nature*, 591 (2021) 482.
11. D. Sun, H. Li, M. Li, C. Li, L. Qian, B. Yang, *Biosens. Bioelectron.*, 132 (2019) 68.
12. M.E. Farias, M.M. Marani, D. Ramirez, A.M. Niebylski, N.M. Correa, P.G. Molina, *Bioelectrochemistry*, 131 (2020) 107397.
13. E. Sundaram, S. Kathiravan, A. Manna, A. Chinnaiyah, V. Vasantha, *ACS Omega*, 4 (2019) 4814.
14. P. Netsuwan, H. Mimiya, A. Baba, S. Sriwichai, K. Shinbo, K. Kato, F. Kaneko, S. Phanichphant, *Sens. Actuators B chem*, 204 (2014) 770.
15. R. Peng, Y. Pan, Z. Li, Z. Qin, J.M. Rini, X. Liu, *Biosen. Bioelectron.*, 197 (2022) 113762.
16. Z.X. Cai, Z.L. Wang, J. Kim, Y. Yamauchi, *Adv. Mater.*, 31 (2019) e1804903.
17. D. Yang, B.C. Gates, *ACS Catal.*, 9 (2019) 1779.
18. Y. Shen, X. Zhong, J. Zhang, T. Li, S. Zhao, B. Cui, D. Wei, Y. Zhang, K. Wei, *Appl. Surf. Sci.*, 498 (2019) 143873.
19. Y. Kim, S. Jang, J.H. Oh, *Microelectron. Eng.*, 215 (2019) 111002.
20. F. Gao, H. Teng, J. Song, G. Xu, X. Luo, *Analytical Methods*, 12 (2020) 604.
21. S.S. Nadar, V.K. Rathod, *Int. J. Biol. Macromol.*, 138 (2019) 1035.
22. X. Chen, S. Xue, Y. Lin, J. Luo, L. Kong, *Anal. Chim. Acta*, 1099 (2020) 94.

23. Z. Altintas, W.M. Fakanya, I.E. Tothill, *Talanta*, 128 (2014) 177.
24. M. Yang, Y. Chen, Y. Xiang, R. Yuan, Y. Chai, *Biosens. Bioelectron.*, 50 (2013) 393.
25. N. Kobayashi, S. Uemura, K. Kusabuka, T. Nakahira, H. Takahashi, *J. Mater. Chem.*, 11 (2001) 1766.
26. T. Al Jishi, C. Sergi, *Reprod. Toxicol.*, 71 (2017) 71.
27. X. Dong, G. Zhao, L. Liu, X. Li, Q. Wei, W. Cao, *Biosens. Bioelectron.*, 110 (2018) 201.
28. M.C. Smith, S. Madec, E. Coton, N. Hymery, *Toxins* (Basel), 8 (2016) 94.
29. H. Zheng, H. Yi, H. Dai, D. Fang, Z. Hong, D. Lin, X. Zheng, Y. Lin, *Sens. Actuators, B*, 269 (2018) 27.
30. P.S. Fontela, J. Papenburg, *The Lancet Infectious Diseases*, 18 (2018) 11.
31. C. Wang, N. Zhang, D. Wei, R. Feng, D. Fan, L. Hu, Q. Wei, H. Ju, *Biosens. Bioelectron.*, 142 (2019) 111521.
32. C. Wang, L. Liu, X. Liu, Y. Chen, X. Wang, D. Fan, X. Kuang, X. Sun, Q. Wei, H. Ju, *Sens. Actuators, B*, 307 (2020) 127619.
33. X. Dong, G. Zhao, X. Li, J. Fang, J. Miao, Q. Wei, W. Cao, *Talanta*, 208 (2020) 120376.
34. G. Zhao, Y. Wang, X. Li, Q. Yue, X. Dong, B. Du, W. Cao, Q. Wei, *Anal. Chem.*, 91 (2019) 1989.
35. G.B. Hu, C.Y. Xiong, W.B. Liang, X.S. Zeng, H.L. Xu, Y. Yang, L.Y. Yao, R. Yuan, D.R. Xiao, *ACS Appl. Mater. Interfaces*, 10 (2018) 15913.
36. D.W. Kufe, *Nature Reviews Cancer*, 9 (2009) 874.
37. G.B. Hu, C.Y. Xiong, W.B. Liang, Y. Yang, L.Y. Yao, W. Huang, W. Luo, R. Yuan, D.R. Xiao, *Biosens. Bioelectron.*, 135 (2019) 95.
38. M. Yan, J. Ye, Q. Zhu, L. Zhu, J. Huang, X. Yang, *Anal. Chem.*, 91 (2019) 10156.
39. C.Y. Xiong, H.J. Wang, W.B. Liang, Y.L. Yuan, R. Yuan, Y.Q. Chai, *Chemistry*, 21 (2015) 9825.
40. D. Tian, H. Zhang, Y. Chai, H. Cui, *Chem. Commun. (Camb)*, 47 (2011) 4959.
41. H.Y. Yang, H.J. Wang, C.Y. Xiong, Y.Q. Chai, R. Yuan, *Biosens. Bioelectron.*, 116 (2018) 16.
42. C. Wang, N. Zhang, Y. Li, L. Yang, D. Wei, T. Yan, H. Ju, B. Du, Q. Wei, *Sens. Actuators, B*, 291 (2019) 319.
43. X. Qin, Y. Dong, M. Wang, Z. Zhu, M. Li, D. Yang, Y. Shao, *ACS Sens.*, 4 (2019) 2351.
44. Q. Liu, Y. Yang, X.-P. Liu, Y.-P. Wei, C.-J. Mao, J.-S. Chen, H.-L. Niu, J.-M. Song, S.-Y. Zhang, B.-K. Jin, M. Jiang, *Sens. Actuators, B*, 242 (2017) 1073.
45. M. Paquette, D. Gauthier, A. Chamberland, A. Prat, E.D. Rolfe, J.J. Rasmussen, L. Kaduka, N.G. Seidah, S. Bernard, D.L. Christensen, A. Baass, *Clin. Biochem.*, 77 (2020) 20.
46. Y. Zhou, J. He, C. Zhang, J. Li, X. Fu, W. Mao, W. Li, C. Yu, *ACS Appl. Mater. Interfaces*, 12 (2020) 338.
47. J.L. Melville, R.G. Compton, *Electroanalysis*, 13 (2001) 123.
48. X.Q. Yang, G.F. Ruan, J.H. Xu, S. Zheng, K. Wang, C.H. Ding, *Clin. Rheumatol.*, 8 (2020) 1663.
49. T.Z. Liu, R. Hu, X. Zhang, K.L. Zhang, Y. Liu, X.B. Zhang, R.Y. Bai, D. Li, Y.H. Yang, *Anal. Chem.*, 88 (2016) 12516.
50. S. Dong, D. Zhang, H. Cui, T. Huang, *Sens. Actuators, B*, 284 (2019) 354.
51. P. Kokoskarova, R. Gulaboski, *Electroanalysis*, 32 (2019) 333.
52. A. Nabers, L. Perna, J. Lange, U. Mons, J. Schartner, J. Güldenhaupt, K.-U. Saum, S. Janelidze, B. Holleccek, D. Rujescu, O. Hansson, K. Gerwert, H. Brenner, *EMBO Mol. Med.* 10 (2018) e8763.
53. J. Han, M. Zhang, G. Chen, Y. Zhang, Q. Wei, Y. Zhuo, G. Xie, R. Yuan, S. Chen, *J. Mater. Chem. B*, 5 (2017) 8330.
54. J. Feng, H. Wang, Z. Ma, *Mikrochim. Acta*, 187 (2020) 95.
55. D. Hui, L. Shanghua, L. Qing, L. Yueyuan, L. Yueyun, Z. Zengdian, *Biosens. Bioelectron.*, 195 (2022) 113648.
56. Z.A. Chen, W. Lu, C. Bao, Q. Niu, X. Cao, H. Wang, R.X. Yao, *Mikrochim. Acta*, 186 (2019) 758.
57. J.S. Daniels, N. Pourmand, *Electroanalysis*, 19 (2007) 1239.
58. M. Beckner, A. Dailly, *Appl. Energy*, 162 (2016) 506.

59. L.H. Wee, S.R. Bajpe, N. Janssens, I. Hermans, K. Houthoofd, C.E. Kirschhock, J.A. Martens, *Chem. Commun. (Camb)*, 46 (2010) 8186.
60. J. Li, J. Xia, F. Zhang, Z. Wang, Q. Liu, *Talanta*, 181 (2018) 80.
61. A. Gupta, S.K. Bhardwaj, A.L. Sharma, K.H. Kim, A. Deep, *Environ. Res.*, 171 (2019) 395.
62. S. Khorrami, M. Tavakoli, E. Safari, *Iran. J. Pathol.*, 14 (2019) 104.
63. C. Zhang, D. Zhang, Z. Ma, H. Han, *Biosens. Bioelectron.*, 137 (2019) 1.
64. C.S. Liu, C.X. Sun, J.Y. Tian, Z.W. Wang, H.F. Ji, Y.P. Song, S. Zhang, Z.H. Zhang, L.H. He, M. Du, *Biosens. Bioelectron.*, 91 (2017) 804.
65. M. Wang, M. Hu, B. Hu, C. Guo, Y. Song, Q. Jia, L. He, Z. Zhang, S. Fang, *Biosens. Bioelectron.*, 135 (2019) 22.
66. I. Helm, L. Jalukse, I. Leito, *Sensors (Basel)*, 10 (2010) 4430.
67. K. Zhang, K. Dai, R. Bai, Y. Ma, Y. Deng, D. Li, X. Zhang, R. Hu, Y. Yang, *Chin. Chem. Letters*, 30 (2019) 664.
68. X. Gao, Y. Zheng, L. Peng, X. Ruan, H. Ji, Y. Qiu, X. Liu, P. Teng, D. Guo, S. Jiang, *Toxicol. In Vitro*, 50 (2018) 190.
69. M. Hu, Y. Wang, J. Yang, Y. Sun, G. Xing, R. Deng, X. Hu, G. Zhang, *Biosens. Bioelectron.*, 142 (2019) 111554.
70. W. Xu, Z. Qin, Y. Hao, Q. He, S. Chen, Z. Zhang, D. Peng, H. Wen, J. Chen, J. Qiu, C. Li, *Biosens. Bioelectron.*, 113 (2018) 148.
71. W. Li, C. Ma, Y. Song, C. Hong, X. Qiao, B. Yin, *Nanotechnology*, 31 (2020) 185605.
72. L. Dai, Y. Li, Y. Wang, X. Luo, D. Wei, R. Feng, T. Yan, X. Ren, B. Du, Q. Wei, *Biosens. Bioelectron.*, 132 (2019) 97.
73. S. Li, S. Yue, C. Yu, Y. Chen, D. Yuan, Q. Yu, *Analyst*, 144 (2019) 649.
74. C.H. Hendon, D. Tiana, A. Walsh, *Phys. Chem. Chem. Phys.*, 14 (2012) 13120.
75. S.K. Bhardwaj, N. Bhardwaj, G.C. Mohanta, P. Kumar, A.L. Sharma, K.H. Kim, A. Deep, *ACS Appl. Mater. Interfaces*, 7 (2015) 26124.
76. S.K. Bhardwaj, A.L. Sharma, N. Bhardwaj, M. Kukkar, A.A.S. Gill, K.-H. Kim, A. Deep, *Sens. Actuators. B*, 240 (2017) 10.
77. J. Liu, Y. Shang, Q. Zhu, X. Zhang, J. Zheng, *Microchim. Acta*, 186 (2019) 509.
78. R.-Y. Bai, K.-L. Zhang, D.-L. Li, X. Zhang, T.-Z. Liu, Y. Liu, R. Hu, Y.-H. Yang, *Chin. J. Anal. Chem.*, 45 (2017) 48.
79. H. Ehzari, M. Amiri, M. Safari, *Talanta*, 210 (2020) 120641.
80. Z. Tang, J. He, J. Chen, Y. Niu, Y. Zhao, Y. Zhang, C. Yu, *Biosens Bioelectron*, 101 (2018) 253-259.
81. M. Zhong, L. Yang, H. Yang, C. Cheng, W. Deng, Y. Tan, Q. Xie, S. Yao, *Biosens. Bioelectron.*, 126 (2019) 493.
82. S. Zhao, Y. Zhang, S. Ding, J. Fan, Z. Luo, K. Liu, Q. Shi, W. Liu, G. Zang, *J. Electroanal. Chem.*, 834 (2019) 33.
83. M. Hu, X. Hu, Y. Zhang, M. Teng, R. Deng, G. Xing, J. Tao, G. Xu, J. Chen, Y. Zhang, G. Zhang, *Sens. Actuators, B*, 288 (2019) 571